SUBJECT: The Increase in Structural Weight
of a Low Cost Expendable Booster
Due to a Lifting Body Payload as
Compared to a Bulbous Payload
Case 105-4

DATE: September 17, 1970

FROM: W. H. Eilertson
C. E. Johnson

ABSTRACT

The TRW low cost launch vehicle (LCLV) study is used
to determine the increase in structural weight associated with
launching a lifting body payload (100 K lbs) into earth orbit
instead of a bulbous payload of the same weight.

Results indicate that low cost launch vehicles (similar
to that studied by TRW) are not adversely affected by the dif-
ference in payload configurations. The structural weight in-
crease is about 2,700 lbs, imposing a payload penalty of about
780 lbs. All of this increase is confined to the forward inter-
stage since the tankage is designed by the high internal operating
pressures associated with pressure-fed propulsion systems, not
flight loads.

Pressure-fed launch vehicles have inherent design
versatility and flexibility since they are relatively insensitive
to payload configurations. Major structural modifications are
not likely to accommodate future payloads as they are identified.

Launch vehicles using pump-fed propulsion systems may
be adversely affected by changing payload configurations since
a larger percentage of the outer wall, involving both tankage
and interstages, has to be modified.

SUBJECT: The Increase in Structural Weight of a Low Cost Expendable Booster Due to a Lifting Body Payload as Compared to a Bulbous Payload Case 105

DATE: September 17, 1970

FROM: W. H. Eilertson
      C. E. Johnson

MEMORANDUM FOR FILE

1.0 INTRODUCTION

Low cost transportation has been identified as the keystone of future large scale space programs (Reference 1). Two obvious ways of achieving this goal exist. One method is to substantially reduce the cost of expendable launch vehicle stages. The other is to recover and reuse the complete system.

The first approach comprises launch vehicles typically characterized by low performance capability due to:

- a lack of sophistication and technology,

- boiler plate construction,

- a minimum amount of avionics,

- pressure-fed engines,

- minimum test and checkout,

and is representative of a launch vehicle system for which engineering refinement is secondary to production cost. The second approach capitalizes on the ability of the aerospace industry to develop and produce high performance equipment which can be recovered and reused. The Space Shuttle, currently under study by NASA, is representative of such a system.

Of the two means for achieving low cost transportation, the Space Shuttle is currently favored by the National Aeronautics and Space Administration. However, the pace of Space Shuttle development, and the technological state of the art may argue for a third or transitional approach that allows partial recovery of space systems. Such a system might be comprised of a recoverable/reusable lifting body payload and an expendable low cost launch vehicle (LCLV). This memorandum deals with the feasibility of such a configuration.

An expendable low cost launch vehicle has been studied by TRW (Reference 2), but only for the case of a

bulbous payload (similar in shape to the Apollo spacecraft), not a lifting body. The feasibility of the transitional approach is dependent on what structural LCLV penalties are incurred by boosting a lifting body payload instead of a bulbous payload. Using the TRW study as a basis, this memorandum gives a preliminary assessment of the relative magnitude of the structural penalties involved. Implications for advanced program planning are also discussed.

2.0 STUDY APPROACH

TRW LCLV interstage weights are scaled to account for changes in flight design loads due to launching a lifting body payload (100 K lbs) into earth orbit instead of a bulbous payload of the same weight. Propulsion tankage comprises the remaining structure and is not affected by changes in flight loadings because pressure-fed propulsion systems are employed in the LCLV as compared to pump-fed systems representative of the Saturn V design. Since pressure-fed propulsion systems are designed with high internal operating pressures (250 psi to 440 psi, Reference 3), the tank walls are more than adequate to withstand flight launch loads (see Appendix A). Moreover, the LCLV is rendered more rigid in bending than a pump-fed propulsion vehicle of the same size.

Flight design loads for both launch vehicle/payload configurations are derived by determining the maximum loading condition resulting from:

1. maximum wind and gust induced loads at maximum dynamic pressure (max q), and

2. maximum longitudinal acceleration at first stage engine cutoff.

A general discussion of these loading conditions is presented below. The detailed analyses are contained in Appendices B and C.

The first loading condition generally occurs in the 25,000 foot to 45,000 foot altitude region where high dynamic pressure and severe wind environments combine to produce the largest loads normal to the vehicle centerline. These normal loads induce large vehicle bending moments which, when combined with existing axial loads, result in net loads that primarily influence the forward portion of the vehicle. This maximum wind response condition is one of the most critical flight conditions for structural design and is particularly significant in the design of launch vehicles used in combination with lifting body payloads.

A max q angle of attack* (α) of 5° occurring at 82 seconds after liftoff and a maximum dynamic pressure (q) of 689 psf have been assumed for this study. An angle of attack of 5° is believed to be reasonable for a lifting body if a wind-biased trajectory is employed similar in nature to that currently proposed for Skylab (Reference 4). However, if a wind-biased trajectory is not used, the angle of attack could possibly be as high as ∿10° (References 5 and 6).

The assumed value for maximum dynamic pressure reflects a payload capability, based on inhouse studies, of ∿100 K lbs into a 100 nm orbit. It accounts for both steady-state and gust wind loadings and is representative of the Saturn V three-stage liquid-propellant launch vehicle (Reference 5). The TRW value of 1050 psf for maximum dynamic pressure (Reference 6) is higher than the assumed value of 689 psf, but the corresponding payload pad of 33,000 lbs (Reference 7) is ample margin for trajectory shaping to provide a max q value more amenable to lifting body payloads and comparable to the Saturn V. The Saturn V max q value is also comparable to other launch vehicles such as the Saturn IB, Titan III-2, Titan III-5, and the Gemini launch vehicle, and therefore represents a more realistic design value for this analysis . An estimation of the variation of possible weight penalties for values of q and α greater than those assumed is presented in Section 5.3.

The loads estimate in this analysis is based on rigid body calculations only. The effects of 1) static booster deflection under rigid body loads, and 2) elastic body dynamic response due to wind gusts are not included. The dynamic loading condition involves a separate flexible body analysis comprising the equations of motion for vehicle elastic bending as well as propellant sloshing. The assumption is made that the LCLV is inherently so stiff that rigid body calculations yield reasonable values for the general purpose of this memorandum.

Max q loads are conservatively based on the use of a constant attitude control law. Changes in angular vehicle orientation due to disturbing winds are corrected by thrust vector control of the first stage engine.

The second loading condition (maximum longitudinal acceleration) occurs just before first stage engine cutoff and produces the largest axial loads on the most portions of the vehicle. It has a great influence on the design of the mid and aft portions of the LCLV. Vehicle weight prior to engine

---

*Angle of attack is the angle between the flight path of the vehicle and its centerline.

cutoff is considerably less than at ignition due to the depletion of first stage propellant. Since thrust is essentially constant during engine burn, axial acceleration increases with time and attains a maximum just before burnout. By the time this condition occurs, the vehicle is almost out of the sensible atmosphere and aerodynamic influences are negligible.

The TRW baseline low cost launch vehicle (Reference 2) is used together with bulbous and lifting body payloads (see Figures 1 and 2). A weight breakdown of the LCLV is listed in Table 1 (Reference 2). Both payloads are 100 K lbs (including the payload/launch vehicle adapter). The bulbous payload, shown in Figure 3, is configured similar to the Apollo spacecraft with an additional section large enough to hold 50 K lbs of hydrogen fuel. The lifting body configuration, shown in Figure 4, is representative of the starclipper as studied by Lockheed (Reference 8). Figure 3 also depicts a typical truss structure which might be used as an adapter for the attachment of the lifting body payload to the LCLV. In addition, an aerodynamic fairing will probably be required.
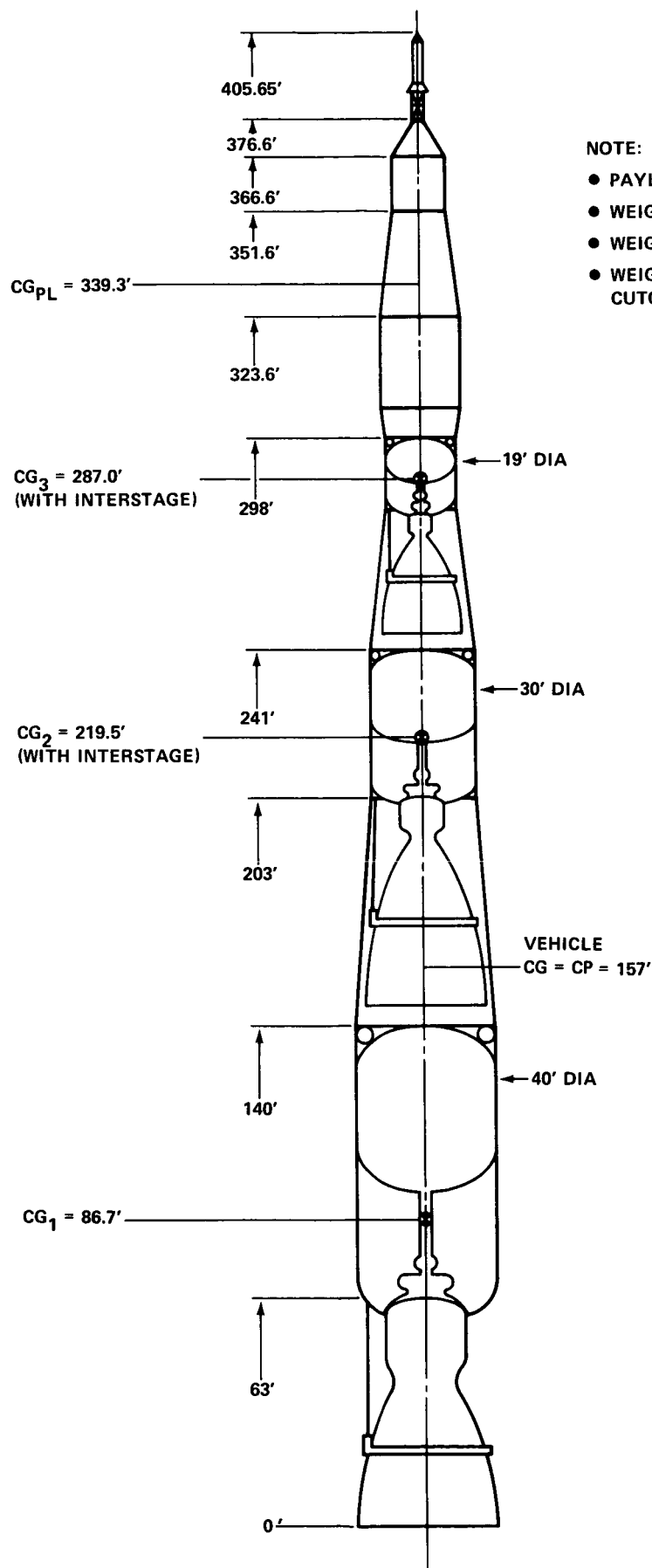
3.0 LCLV WITH BULBOUS PAYLOAD

3.1 Max q Loads

Figure 1 depicts the LCLV/bulbous payload configuration. The payload and LCLV adapter weigh 100 K lbs. At max q the total vehicle weighs about 4.9 M lbs. The vehicle center of gravity and center of pressure are approximately coincident (157 ft above the base of the first-stage engine). Because of this, the vehicle is neutrally stable and thrust vector control does not have a first-order effect on the bending analysis.

Figure 5 contains a plot of aerodynamic moments* and relieving inertia moments for the total launch vehicle at max q. The resulting moment at any station cross-section is equal to the difference of the two curves. Notice that bending moments are relatively large at the aft end of the vehicle. This is primarily due to the small amount of mass contained in this section of the vehicle; that is, the very large but "empty" first-stage engine and the partially depleted first-stage propulsion tankage. The bending moment at the base of the bulbous payload is about 2.1×10^6 ft lbs.
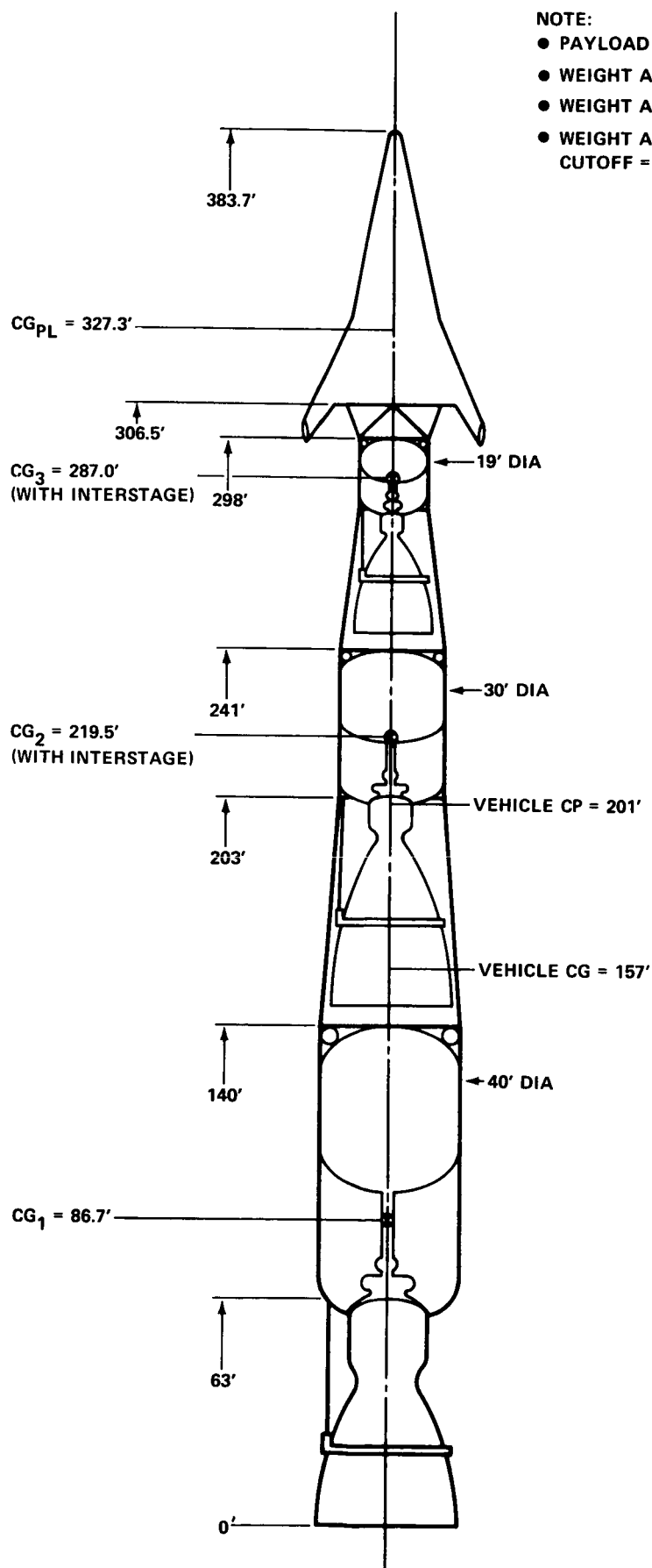
---

*Computed bending moments involve the subtraction of inertia relief moments from aerodynamic moments. Since the magnitudes of these moments are very large and the differences small, the accuracy may not be adequate for calculations other than the estimations contained in this memorandum.

NOTE:
- PAYLOAD = 100,000 LBS
- WEIGHT AT LIFTOFF = 9,237,082 LBS
- WEIGHT AT MAX q = 4,887,082 LBS
- WEIGHT AT FIRST STAGE ENGINE CUTOFF = 2,999,320 LBS

405.65'
376.6'
366.6'
351.6'
CG_{PL} = 339.3'
323.6'
CG_3 = 287.0' (WITH INTERSTAGE)
298'
19' DIA
CG_2 = 219.5' (WITH INTERSTAGE)
241'
30' DIA
203'
VEHICLE CG = CP = 157'
140'
40' DIA
CG_1 = 86.7'
63'
0'

FIGURE 1 - LCLV CONFIGURATION WITH BULBOUS PAYLOAD

NOTE:
- PAYLOAD = 100,000 LBS
- WEIGHT AT LIFTOFF = 9,237,082 LBS
- WEIGHT AT MAX q = 4,887,082 LBS
- WEIGHT AT FIRST STAGE ENGINE CUTOFF = 2,999,320 LBS

383.7'

CG_{PL} = 327.3'

306.5'

CG_3 = 287.0'
(WITH INTERSTAGE) 298'

19' DIA

241'

30' DIA

CG_2 = 219.5'
(WITH INTERSTAGE)

VEHICLE CP = 201'

203'

VEHICLE CG = 157'

140'

40' DIA

CG_1 = 86.7'

63'

0'

FIGURE 2 - LCLV WITH LIFTING BODY PAYLOAD

TABLE I

LCLV WEIGHT BREAKDOWN

ITEM	STAGE 1	STAGE 2	STAGE 3
	WEIGHT (LBS)	WEIGHT (LBS)	WEIGHT (LBS)
TANKS AND SKIRTS	480,167	127,237	25,994
ENGINES AND VALVES	100,483	23,655	6,132
LITVC SYSTEM	12,475	3,153	646
PRESSURIZATION SYSTEM	18,713	3,153	646
ROLL & ULLAGE CONTROL SYSTEM	1,247	315	193
INTERSTAGE (ABOVE)	84,884	14,122	--
PROPELLANT	6,237,762	1,576,735	323,097
ASTRIONICS	2,099	529	693
CONTINGENCY	73,994	18,958	--
TOTAL STAGE WEIGHT	7,011,824	1,767,857	357,401

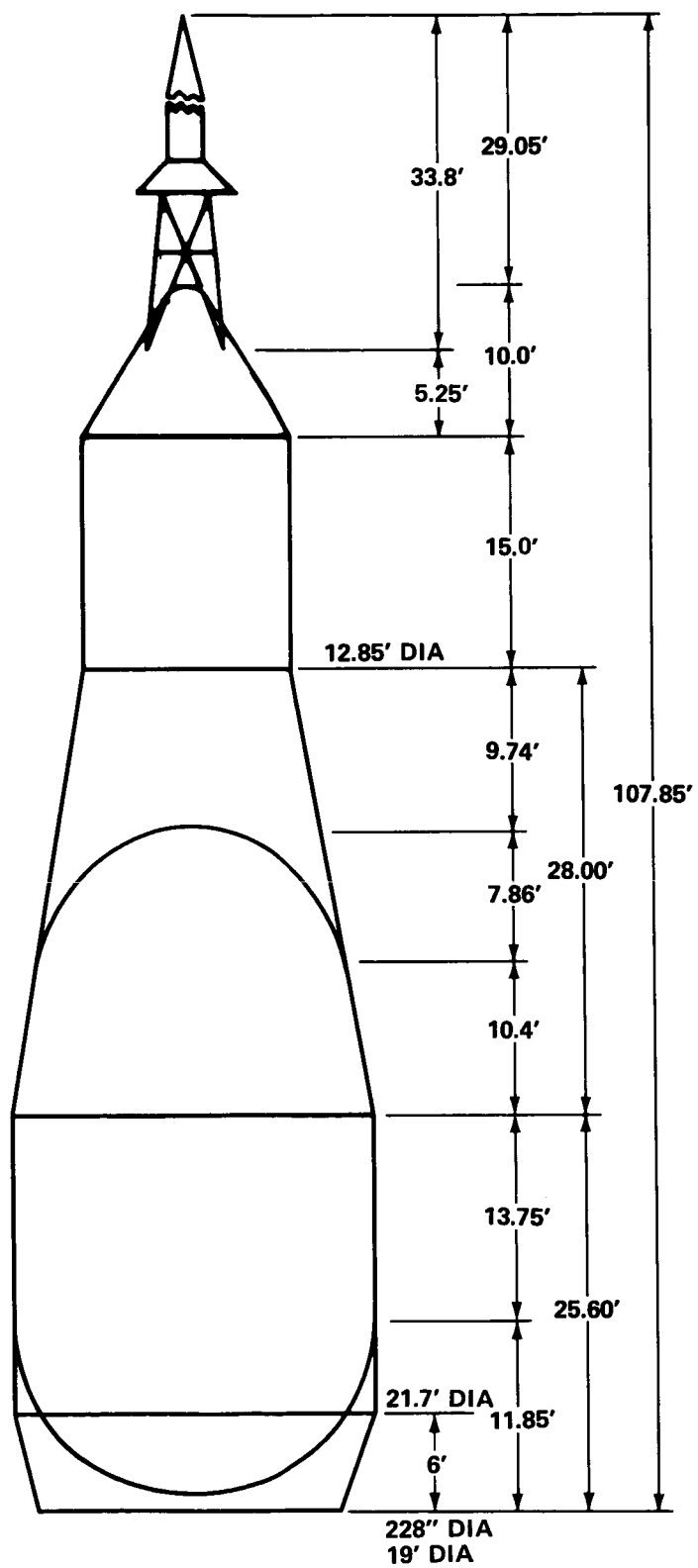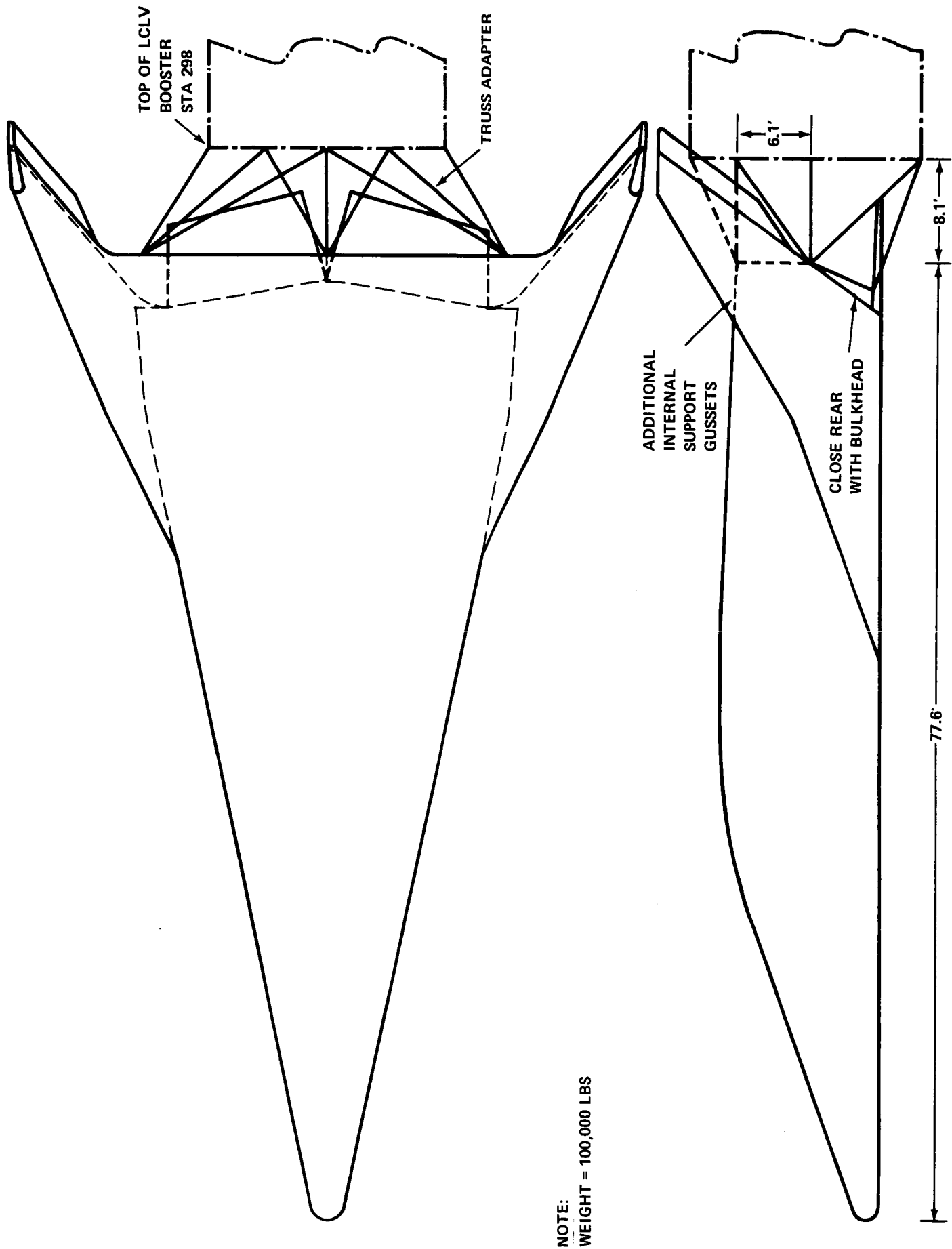NOTE: TOTAL LAUNCH VEHICLE WEIGHT = 9,137,082 LBS

29.05'

33.8'

10.0'

5.25'

15.0'

12.85' DIA

9.74'

107.85'

28.00'

7.86'

10.4'

13.75'

25.60'

21.7' DIA   11.85'

6'

228" DIA
19' DIA

NOTE:

WEIGHT = 100,000 LBS

FIGURE 3 - BULBOUS PAYLOAD CONFIGURATION

TOP OF LCLV
BOOSTER
STA 298

TRUSS ADAPTER

ADDITIONAL
INTERNAL
SUPPORT
GUSSETS

CLOSE REAR
WITH BULKHEAD

6.1'

8.1'

77.6'

NOTE:
WEIGHT = 100,000 LBS

FIGURE 4 - LIFTING BODY CONFIGURATION ILLUSTRATING A TYPICAL TRUSS ADAPTER
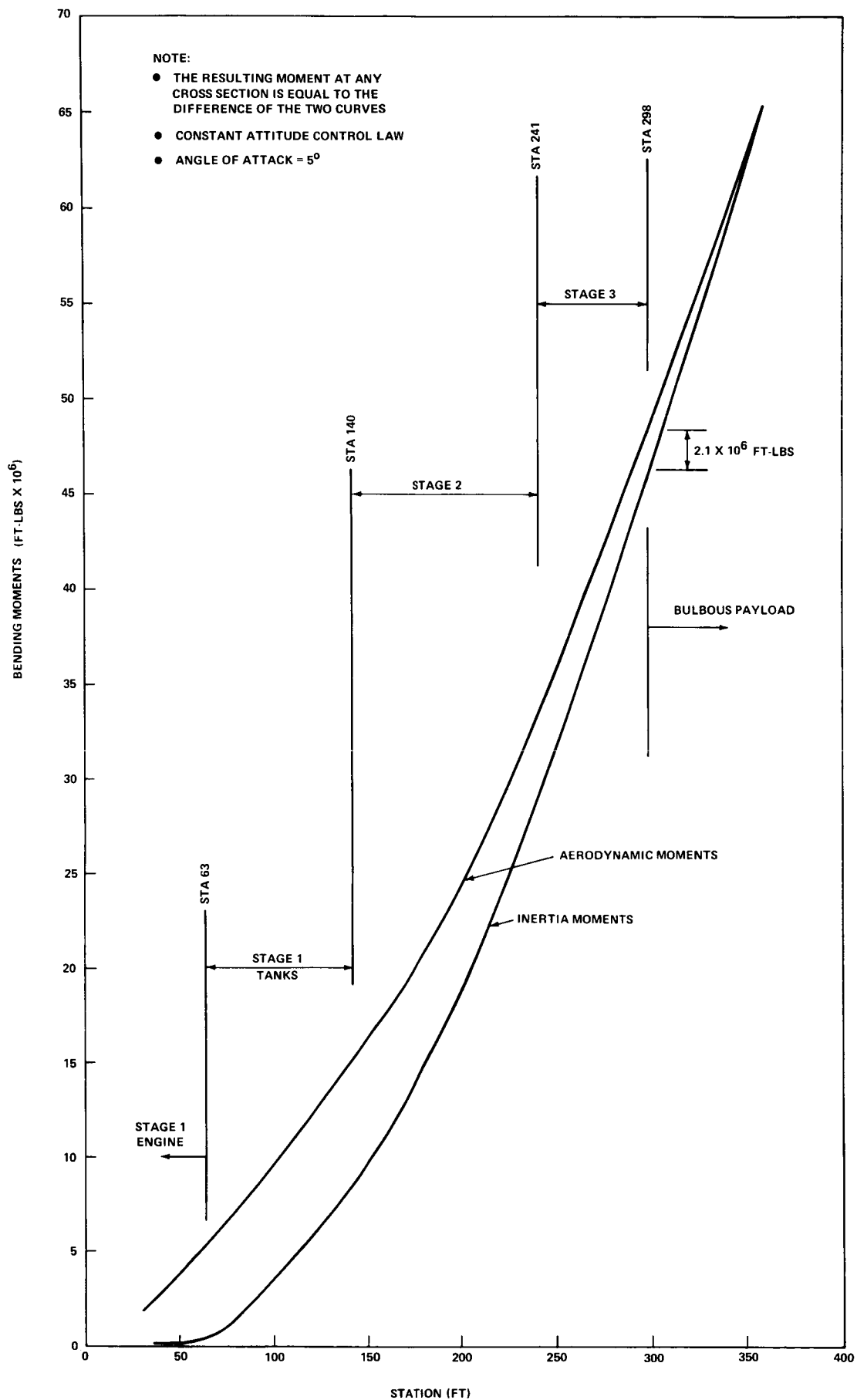
FIGURE 5 - AERODYNAMIC AND INERTIA - RELIEF MOMENTS FOR THE LCLV WITH A BULBOUS PAYLOAD AT MAX q

Figure 6 contains a plot of axial inertia and drag loads for the total launch vehicle at max q. Notice that the relative effect of drag loading is almost negligible at the base of the vehicle but is substantial at the forward end.

3.2 Maximum Longitudinal Loads

Figure 7 contains a plot of the maximum longitudinal launch vehicle loading experienced just before first-stage engine cutoff. This figure applies for both the bulbous and the lifting body launch-vehicle/payload configurations since both payloads are equal in weight and are out of the sensible atmosphere. At this point in the trajectory the total vehicle weighs about 3 M lbs. The flat portions of the plot correspond to interstages and the steep portions to the propulsion systems. It is seen that the first-stage tankage loading is not as steep as for the second and third stages. This is due to the depleted state of first-stage propellant at this point in the trajectory.

3.3 LCLV Flight Design Loads for a Bulbous Payload

Figure 8 contains plots of 1) equivalent axial running loads (P_{eq}) for the max q loading condition and 2) axial running loads for the maximum longitudinal loading condition. It is seen that the maximum longitudinal loading condition determines the structural flight design loads at all LCLV stations. This conclusion is in accordance with TRW studies (Reference 6).

4.0 LCLV WITH LIFTING BODY PAYLOAD

Figure 4 depicts the LCLV lifting body payload configuration. Weight histories are assumed the same for both the lifting body and bulbous payload cases.

4.1 Max q Loads

The vehicle center of gravity (CG) is 157 ft above the base of the first-stage engine (the same as for the bulbous payload), whereas the vehicle center of pressure (CP) is 201 ft above the base. Since the CP is forward of the CG, the vehicle is statically unstable and thrust vector control of the first-stage engine must compensate for the tendency of the vehicle to rotate to large angles of attack when flying through winds. Therefore, thrust vector bending moments were included in this analysis. Note that in the previous section (3.0) no thrust vector bending moments were included in the analysis since the bulbous-payload/launch-vehicle configuration was neutrally stable.
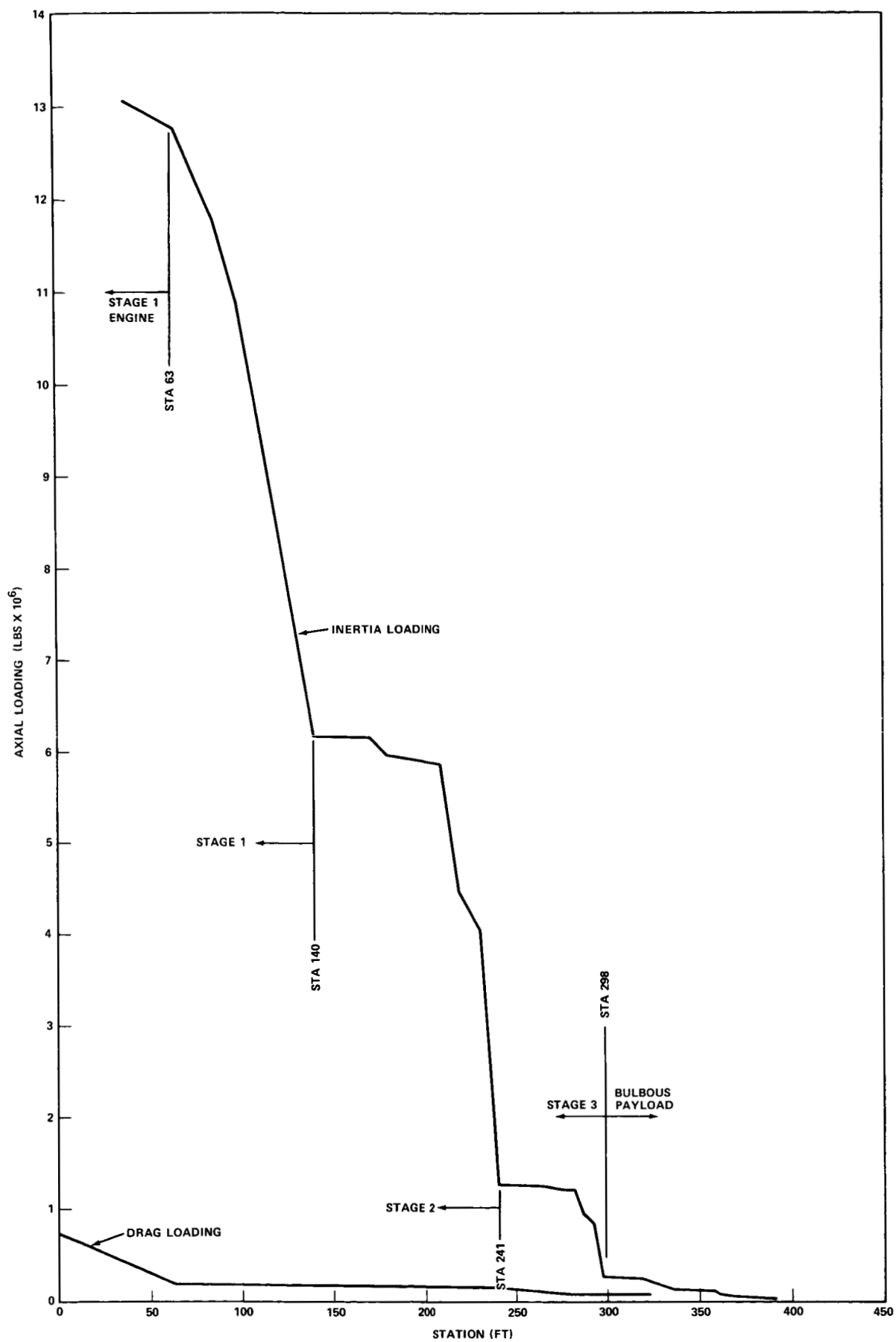
FIGURE 6 - AXIAL INERTIA AND DRAG LOADS FOR THE LCLV WITH A BULBOUS PAYLOAD AT MAX q
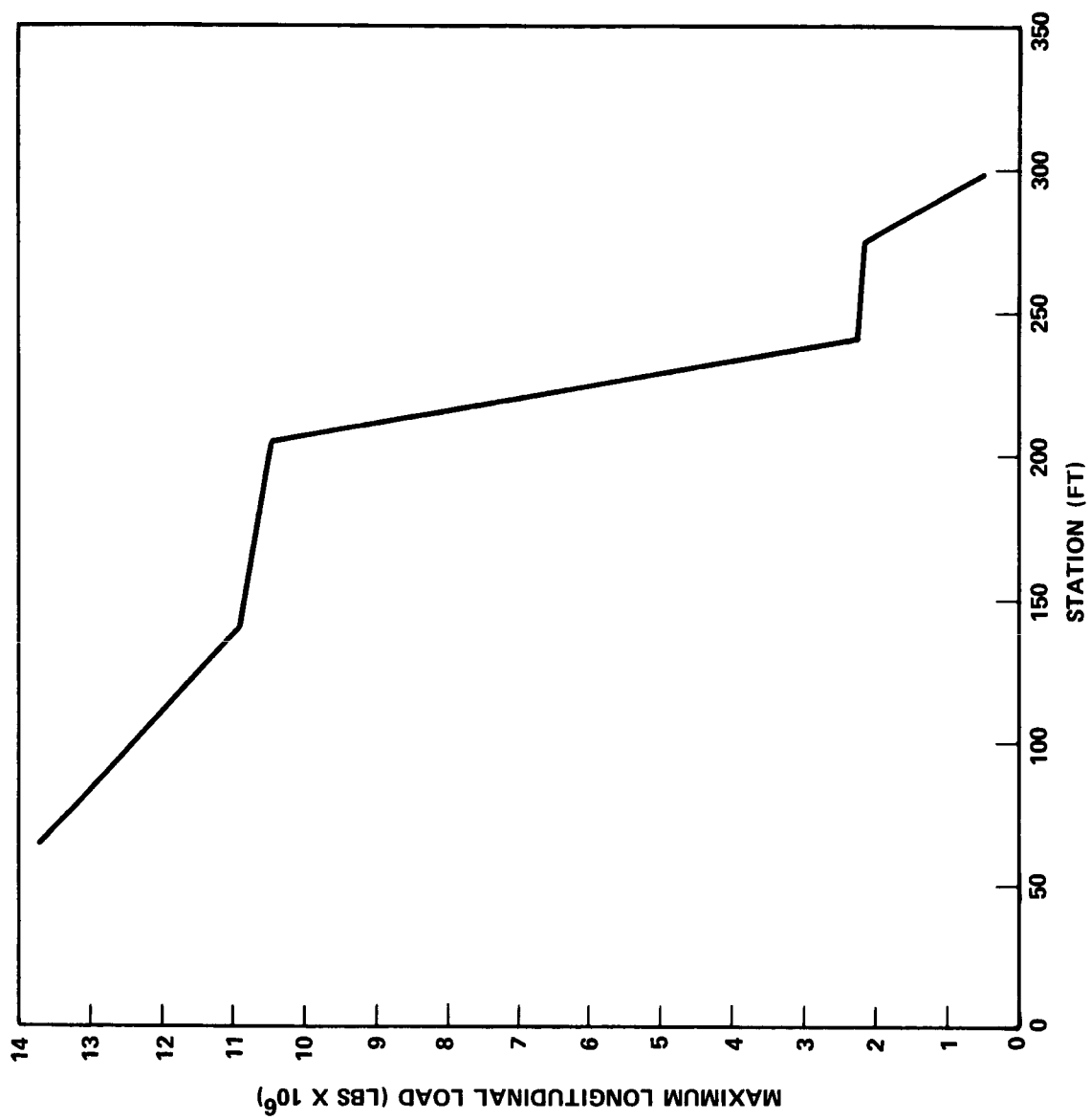
FIGURE 7 - MAXIMUM LONGITUDINAL LOAD FOR A LCLV WITH A 100 K-LB PAYLOAD
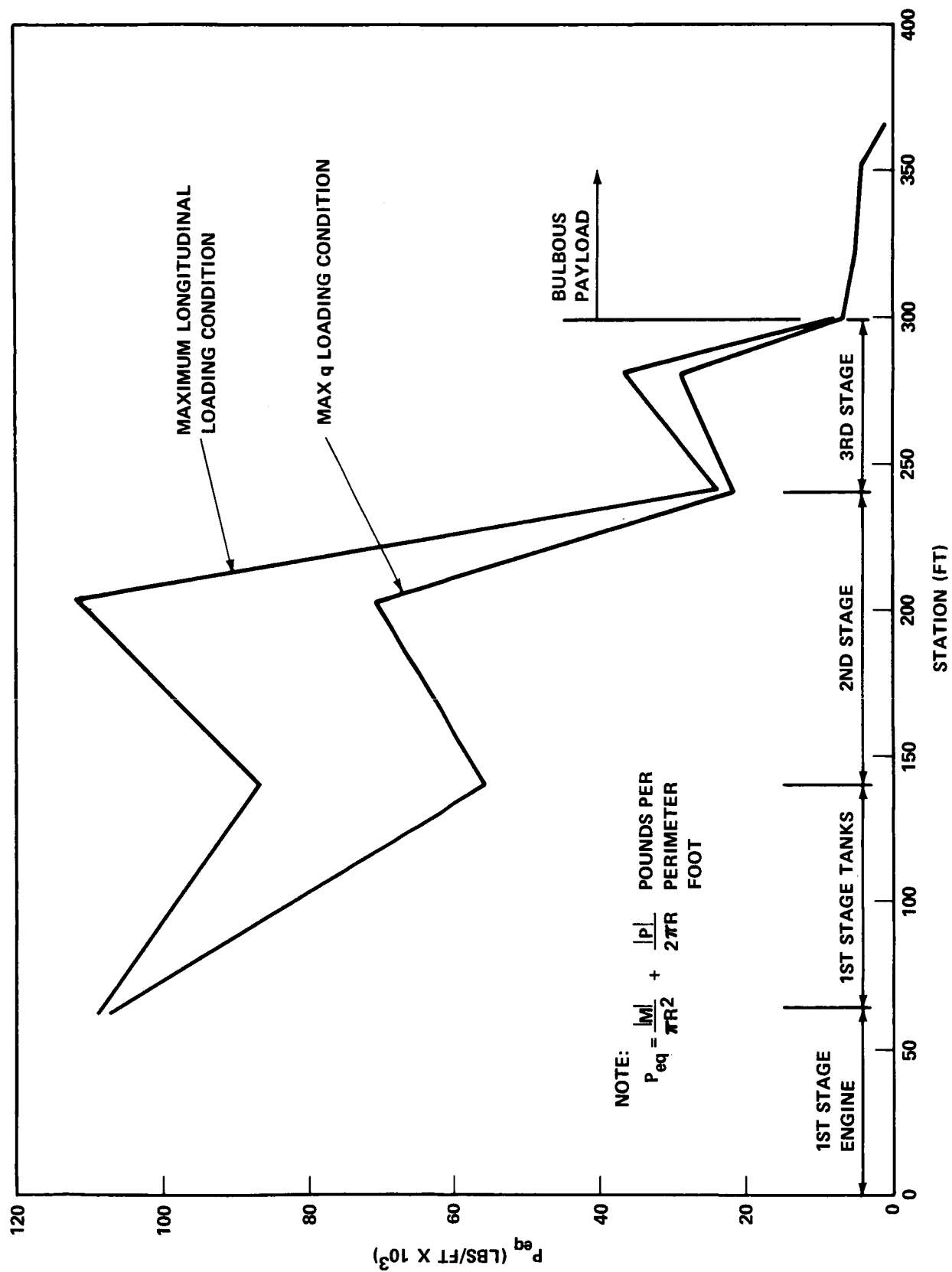(PRIOR TO FIRST STAGE ENGINE CUTOFF)

FIGURE 8 - AXIAL RUNNING LOADS FOR A LCLV WITH A BULBOUS PAYLOAD

Figures 9 and 10 are plots of vehicle bending moments and axial loads similar to Figures 5 and 6. It is seen that the bending moment at the payload base for the lifting body is 3.7×10^6 ft lbs, about a factor of 1.8 greater than that for a bulbous payload. Axial loads remained essentially the same.

4.2 Maximum Longitudinal Loads

The maximum longitudinal launch loads experienced by the LCLV just before first stage engine cutoff with a lifting body payload are the same as for the bulbous payload. This loading condition is shown in Figure 7.

4.3 LCLV Flight Design Loads for a Lifting Body Payload

Figure 11 contains plots of 1) equivalent axial running loads (P_{eq}) for the max q loading condition and 2) axial running loads for the maximum longitudinal loading condition. It is seen that the maximum longitudinal loading condition determines flight design loads for the mid and aft portions of the vehicle, whereas the max q loading condition determines flight design loads for the forward portion of the vehicle above Station 233.

Comparing Figure 11 with Figure 8 it is seen that launching a lifting body payload instead of a bulbous payload only affects the forward end of the LCLV above Station 233. Structural flight design loads remain the same for the mid and aft portions of the launch vehicle.

5.0 STRUCTURAL WEIGHT PENALTIES

The forward interstage and propulsion tankage for Stages 2 and 3 are included in the forward end of the LCLV above Station 233. The structural weight of the interstage must be increased since it is designed by flight launch loads. However, the structural weight of the propulsion tankage does not change since it is designed by the internal operating pressures associated with the pressure fed engines (see Section 2.0).

5.1 Increase in Structural Weight of Forward Interstage

Theoretically, structures like interstages should be designed so that maximum stresses and buckling loads occur simultaneously. If this were so, the TRW interstage weight listed in Table 1 could be scaled directly with the equivalent axial running load (P_{eq}). However, practically speaking, this is not the case for the LCLV since other design factors such as
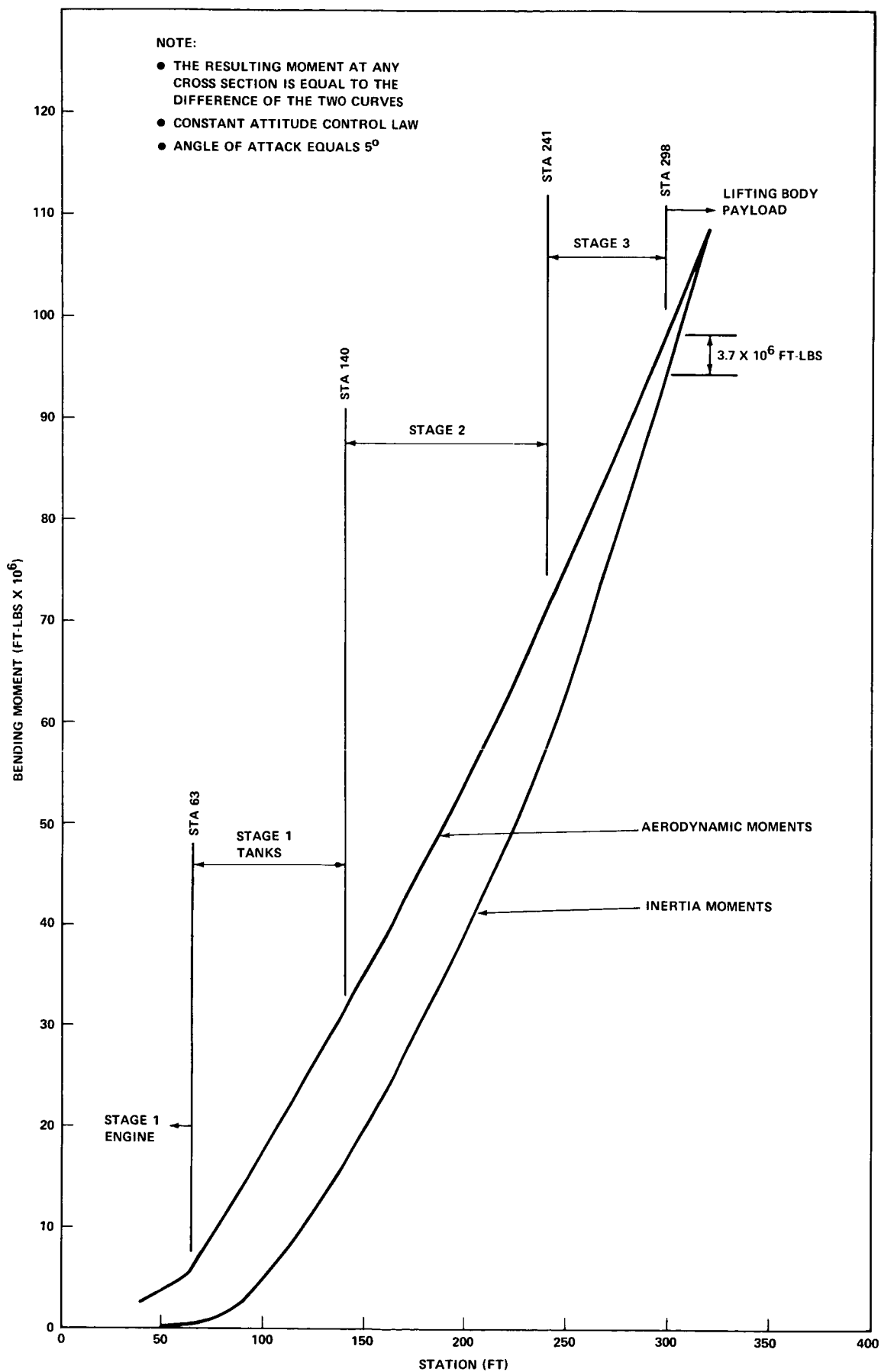
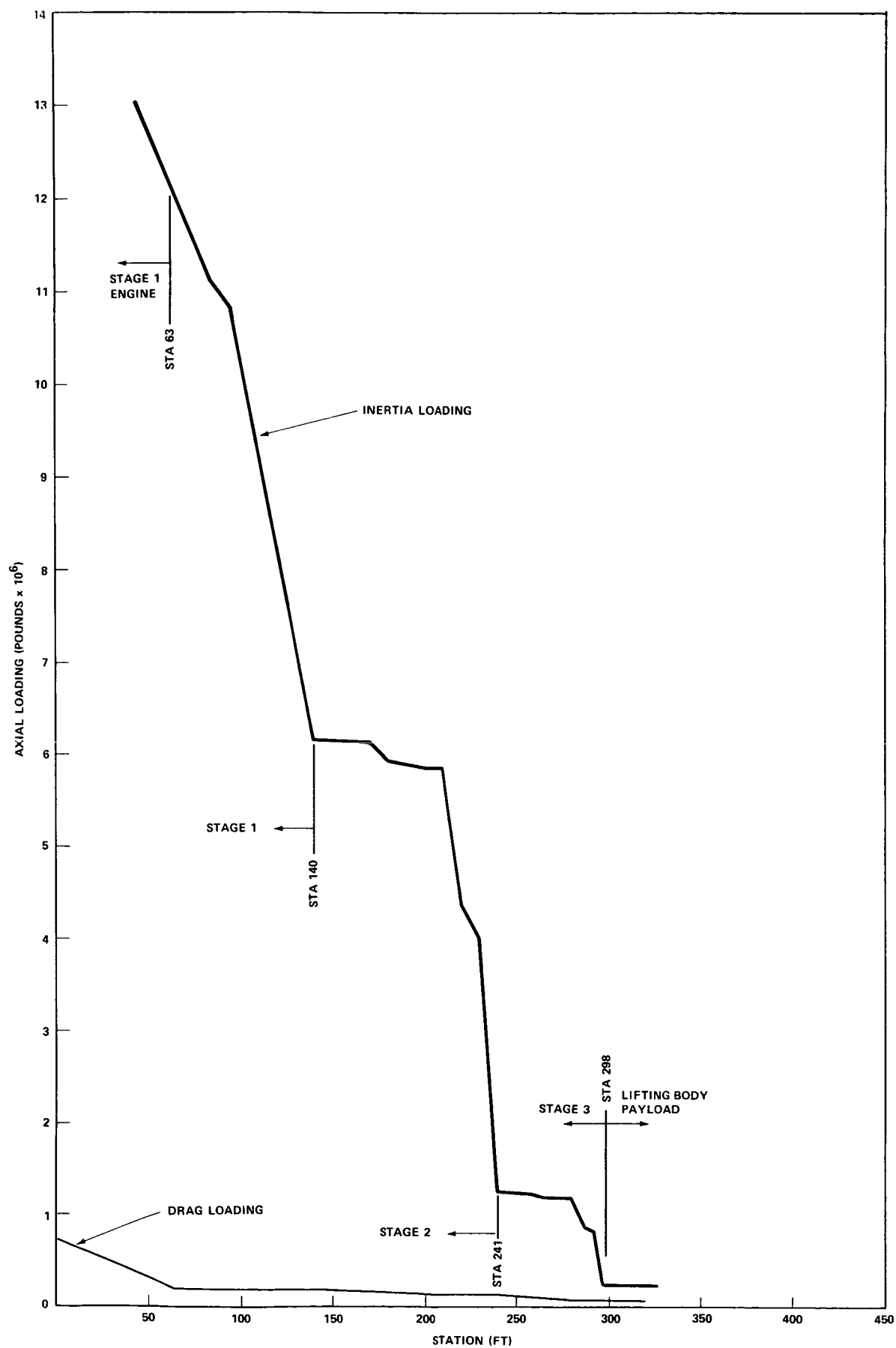FIGURE 9 - AERODYNAMIC AND INERTIA-RELIEF MOMENTS FOR THE LCLV WITH A LIFTING BODY PAYLOAD AT MAX-q

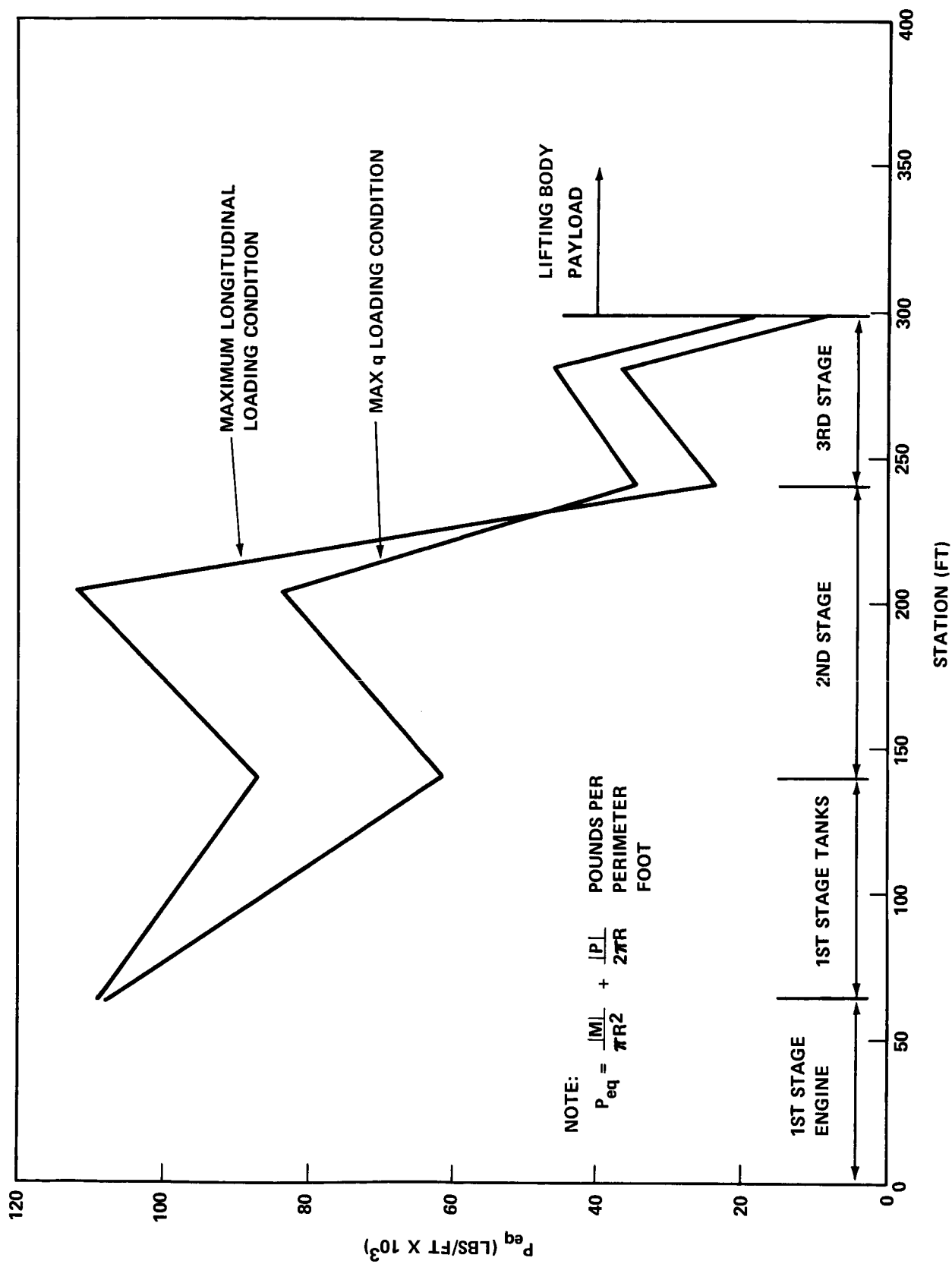FIGURE 10 - AXIAL INERTIA AND DRAG LOADS FOR THE LCLV WITH A LIFTING BODY PAYLOAD AT
MAX-q

FIGURE 11 - AXIAL RUNNING LOADS FOR A LCLV WITH A LIFTING BODY PAYLOAD

manufacturing costs, minimum gages, etc., must also be considered. Dr. Kaplan of TRW (cognizant of the LCLV structural design) was consulted to obtain the appropriate scaling law to use. Based on these discussions and Reference 6, interstage weight (W_i) varies with P_{eq} as

$$W_i \propto P_{eq}^{6/10}. \tag{1}$$

Using Equation (1), Table 1, and Figure 11, the interstage weight for a lifting body payload (W_i^*) can be estimated using the scaling equation

$$W_i^* = W_i \left(1 + \frac{\text{\% Average Increase in } P_{eq}}{100} \right)^{6/10} \tag{2}$$

where

$$W_i = 14,122 \text{ lbs, and}$$

$$\text{\% Average Increase in } P_{eq} = 33.3.$$

Substituting these values into Equation (2), the revised forware interstage weight for a lifting body payload is $W_i = 16,780$ lbs.

The increase in LCLV structural weight due to launching a lifting body payload into earth orbit as compared to a bulbous payload is equal to the difference in forward interstage weights, or

$$\text{Increase in LCLV}$$
$$\text{Structural Weight} = 2,658 \text{ lbs.}$$

5.2 Payload Penalty

The required increase in structural weight of the forward interstage imposes a payload weight penalty for the three-stage TRW LCLV. The analysis of this payload penalty is contained in Appendix C. It is determined that an increase of 2,658 lbs in forward interstage weight reflects as a payload penalty of 780 lbs or 0.78 percent.

5.3 Sensitivity of Structural Weight Penalties to Variations in q and α for a Lifting Body Payload

Inhouse studies have shown that the payload capability of the LCLV is $\gtrsim$ 100 K lbs at a maximum dynamic pressure of 689 psf. Structural weight penalties were estimated using this value for q and an

angle of attack of 5°. If the values for q and α are actually greater than these values for the trajectory considered, the associated weight penalties increase.

Figures 12 and 13 depict weight increases for values of q between 689 psf and 1100 psf, and values of α between 5° and 10°. The upper limits for these parameters are in accord with Section 2.0 of this memorandum and represent worst-case possibilities. That is, the need for flying lifting-body missions with maximum dynamic pressures as great as 1100 psf appears remote. Furthermore, a requirement to withstand angles of attack as great as 10° when less than this can now be achieved is also improbable. The structural capability of the upper interstage needs to be increased for all the combinations of q and α considered. However, above certain values of q and α the lower interstage weight must also be increased, and this is the reason for the breaks and slope changes in the curves. The payload penalty equation in Appendix D was modified to reflect the increasing of lower interstage weights.

It is seen that the LCLV structural weight penalties could vary between 2,700 lbs and 35,000 lbs with a corresponding range of payload penalties between 780 lbs and 6,260 lbs. Although these ranges are extensive, they do not appear to be significant when compared to a 100 K lb payload capability. Moreover, if trajectory modifications are considered, it is possible that increases in available payload capability might offset the actual penalties involved.

6.0 IMPLICATIONS FOR ADVANCED PROGRAM PLANNING

The block diagram shown in Figure 14 illustrates the various configuration alternatives that are available when considering the use of expendable launch vehicles in advanced program planning. Bulbous or lifting body payloads can be launched with pressure-fed LCLV's or with launch vehicles employing pump-fed propulsion systems.

Pressure-fed LCLV's offer inherent design versatility and flexibility to the advanced program planner since they are relatively insensitive to payload configurations. Little additional structural weight is required and changes are confined primarily to the forward interstage. Therefore, major structural modifications to existing structure are not required to accommodate payload requirements as they are identified. This characteristic is notable since it is primary to the selection of future space systems.

The same cannot be said for pump-fed launch vehicles. Internal operating pressures for pump-fed propulsion systems are around 30 psi to 40 psi as compared to 250 psi to 440 psi for the TRW LCLV. Therefore, the tankage outerwall structure of
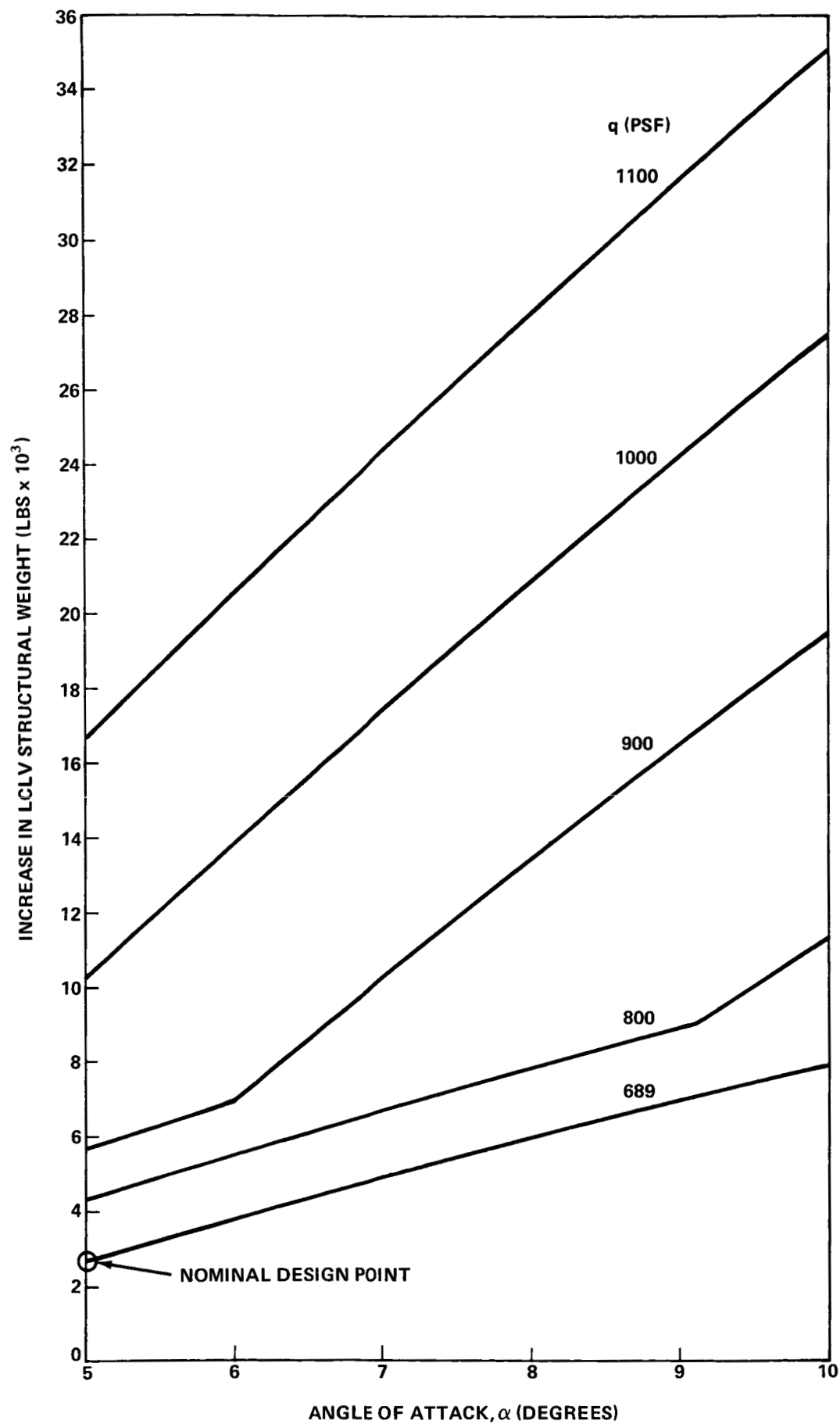
FIGURE 12 - LCLV STRUCTURAL WEIGHT PENALTY VERSUS α AND q FOR A
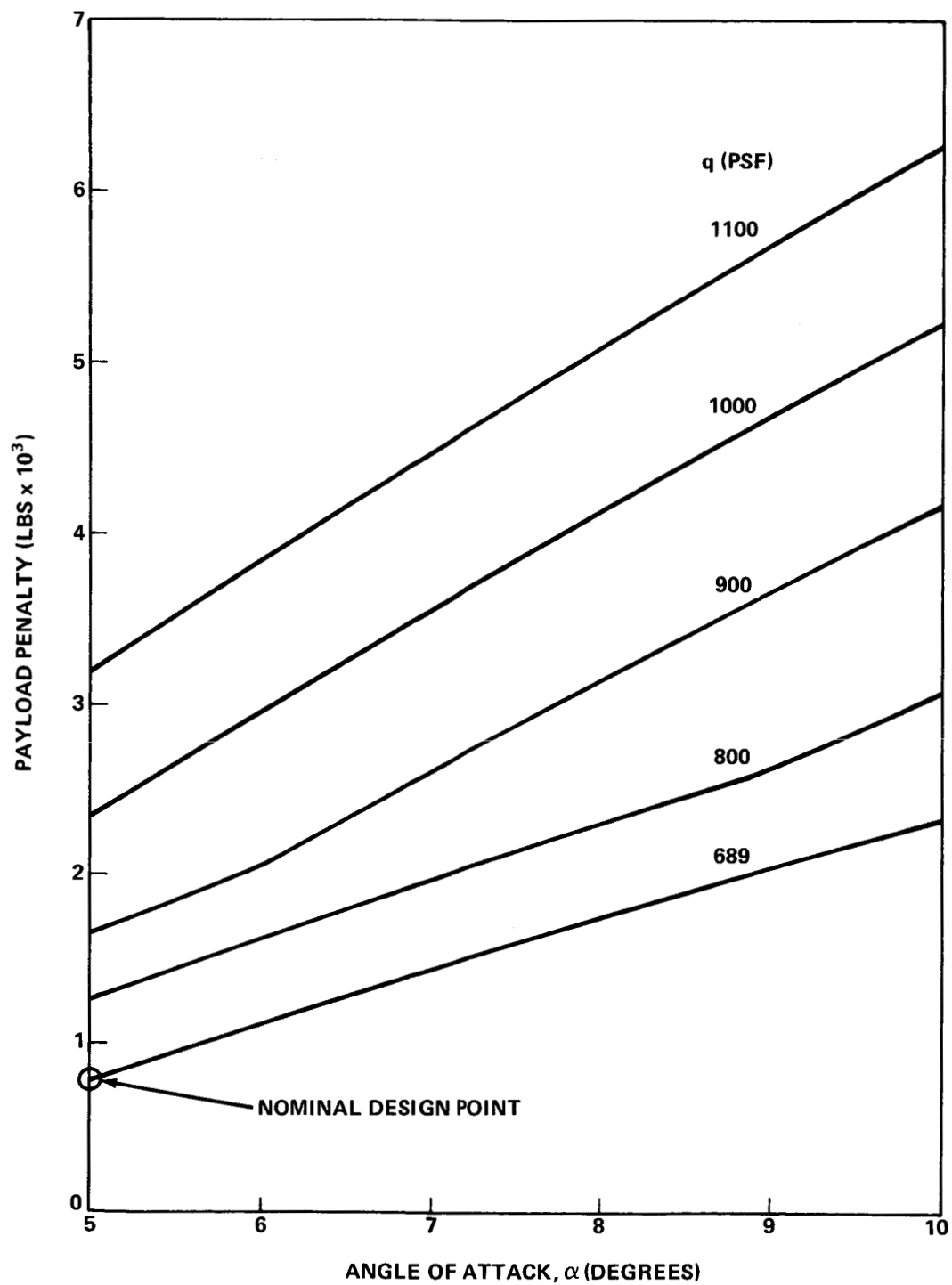100 K-LB LIFTING BODY PAYLOAD

FIGURE 13 - PAYLOAD PENALTY VERSUS α AND q FOR A LCLV WITH A
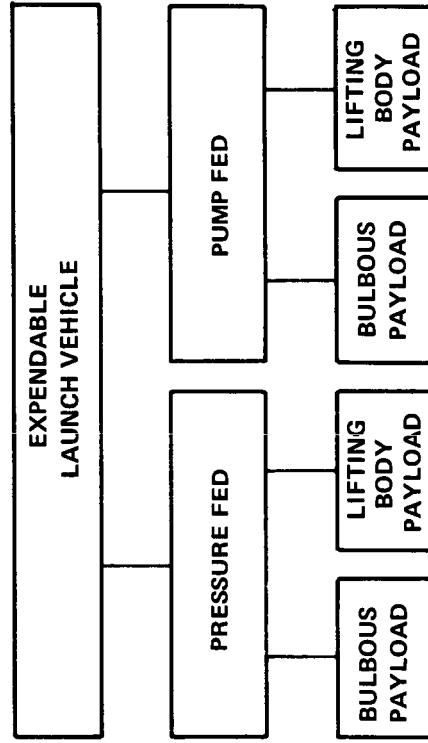100 K-LB LIFTING BODY PAYLOAD

FIGURE 14 - LAUNCH VEHICLE/PAYLOAD CONFIGURATION
ALTERNATIVES FOR ADVANCED PLANNING

these vehicles (Saturn V, Agena, Atlas, etc.) is designed by flight loads, not by propulsion system pressures. It has been shown that flight loads are a function of the payload and launch vehicle configurations. Moreover, since pump-fed vehicles are inherently more flexible, they are subject to additional quasi-static and dynamic loads that pressure-fed vehicles are not subject to. Consequently, launch vehicles using pump-fed propulsion systems may be adversely affected by payload configuration requirements since a larger percentage of the outer wall, involving propulsion tankage as well as interstages, has to be modified.
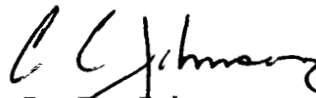
The gross weight and size of a three-stage pump-fed launch vehicle required to place a 100 K lb payload into earth orbit differs substantially from that representative of the LCLV studied in this memorandum. Therefore, this analysis cannot be directly applied to determine corresponding weight penalties for comparison. A separate study is required to establish these penalties and is not included herein.

7.0 CONCLUSIONS

- Pressure-fed launch vehicles tend to be insensitive to varying payload configurations. Major structural modifications are not required.

- The LCLV structural weight must increase by about 2,700 lbs to launch a 100 K lbs lifting body payload into earth orbit instead of a bulbous payload of the same weight. The associated payload penalty is about 780 lbs.

- All of this weight penalty is confined to the forward interstage (between the second and third propulsion stages) since the tankage is designed by the high internal operating pressures associated with pressure-fed propulsion systems, not flight loads.

W. H. Eilertson

C. E. Johnson

1012-$\frac{WHE}{CEH}$-pak

BELLCOMM, INC.

REFERENCE

1. NASA Science and Technology Advisory Committee for Manned
    Space Flight, Proceedings of the Winter Study on Uses of
    Manned Space Flight, 1975-1985, Volume II, Appendices,
    Appendix A, NASA SP-196.

2. "Low Cost Launch Vehicle Study," Midterm Report, 11851-
    6003-RO-OO, TRW Systems Group, Redondo Beach, California,
    December 1968.

3. Kaplan, A., "Structural Considerations for LCLV Propellant
    Tanks," Interoffice Correspondence to J. B. Kendrick,
    69-4340.3-9, TRW Systems Group, March 26, 1969.

4. Technical Discussions with R. Hunter of Bellcomm, Inc.,
    July 22, 1970.

5. "CSM Technical Specification, Block II," January 1, 1968,
    SID 64-1344B, North American Rockwell.

6. Kaplan, A., "Weight Equations and Design of the LCLV
    Interstage Structures," Interoffice Correspondence
    J. B. Kendrick, 69-4340.3-6, TRW Systems Group, March 13,
    1969.

7. "Low Cost Launch Vehicle Study", Final Report, 11851-
    6010-RO-OO, TRW Systems Group, Redendo Beach, California,
    June, 1969.

8. "Space Transport and Recovery System," Lockheed Missiles
    and Space Company, LMSC-A914691, February 1, 1968, (U)
    CONFIDENTIAL.

9. USAF Stability and Control DATCOM, Flight Control Division,
    Air Force Flight Dynamics Laboratory, Wright-Patterson Air
    Force Base, Ohio, July, 1963.

BELLCOMM, INC.

APPENDIX - A

CAPABILITY OF TANK WALLS TO WITHSTAND
FLIGHT LAUNCH LOADS

LCLV pressure-fed propulsion tankage are more than adequate to withstand flight launch loadings since they are designed to high internal operating pressures (250 psi to 440 psi) as compared to operating pressures for pump-fed systems (30 psi to 40 psi). A very high tension state of prestress exists in the longitudinal direction which obviates buckling failure. Also, since the longitudinal stress is one half the design hoop tensile stress, a large strength reserve exists to account for vehicle-bending tensile stresses at max q.

Table A-1 compares the maximum expected flight launch loads at first stage engine cutoff and at max q with longitudinal tankage loading conditions due to internal pressure. It is seen that the prestressed tension state of the cylindrical tank walls is on the order of an order-of-magnitude higher than flight compression loads at either first stage engine cutoff or max q, thereby negating tankage failure due to buckling. Also, it is seen that flight tensile loadings at max q due to booster bending are negligable when compared to the additional tensile capability available.

TABLE A-1 LCLV TANKAGE LOADING CONDITIONS

TANK	RADIUS (FT)	THICKNESS (IN)	OPERATING PRESSURE (PSI)	ULTIMATE PRESSURE (PSI)	CYLINDER LONGITUDINAL DESIGN RUNNING LOADS (LBS/FT x 10^3)				
					INTERNAL PRESSURE (TENSION)	ADDITIONAL CAPABILITY (TENSION)	FLIGHT LAUNCH LOADS		
							1st STAGE ENGINE CUTOFF (COMP)	MAX q	
								(COMP)	(TENS)
STAGE 3									
OXIDIZER	9.5	0.416	340	510	348.5	348.5	16	25	7.4
FUEL	9.5	0.306	250	375	256	256	31	40	3.4
STAGE 2									
OXIDIZER	15.0	0.752	390	585	632	632	48.5	48.5	0
FUEL	15.0	0.579	300	450	485	485	88	70	0
STAGE 1									
OXIDIZER	20.0	1.131	440	660	950	950	97	82.2	0
FUEL	20.0	0.900	350	525	756	756	107	103.5	0

BELLCOMM, INC.

APPENDIX B

ANALYSIS OF MAXIMUM WIND AND GUST INDUCED LOADS

1.0 RIGID BODY LOADS

The rigid body loads induced at max-q comprise bend-
ing moments, shears, axial loads, and the associated load
factors. In order to calculate these quantities, the equations
of motion must be determined and certain definitions established.
In this analysis, it is assumed that the vehicle maintains con-
stant attitude during max q wind loading, requiring rotation of
the thrust vector to prevent vehicle rotation.*

1.1 Equations of Motion

A free body diagram of the total launch vehicle in
flight at max q is shown in Figure B-1. The coordinate system
as well as the sign convention employed is indicated. This sys-
tem utilizes a three degree of freedom coordinate system for
simplicity; the three degrees being two translatory and one
rotational. The positive sign convention is shown for the exter-
nal forces and the internal loading.

The nomenclature used in this analysis is presented
below:

Symbol	Description	Units
$r(x)$	Distance from missile center of gravity to station x	in
δ	Thrust vector angle	Degrees
Θ	Angle between missile longitudinal centerline and horizontal axis of inertia	Degrees
Φ	Angle between vertical axis of inertia reference and radius vector to missile center of gravity from origin of inertial reference	Degrees

---

*LCLV thrust vector control is accomplished by means of
liquid injection so that actual gimballing of the first stage
engine is not required.

FIGURE B-1 - FREE BODY DIAGRAM OF LAUNCH VEHICLE WITH COORDINATE SYSTEM

BELLCOMM, INC.

Symbol	Description	Units
L_{CP}	Distance from center of pressure to center of gravity	in
L_E	Distance from engine gimbal station to center of gravity	in
$\ddot{x}$	Longitudinal acceleration of the center of gravity	in/sec^2
$\ddot{y}$	Normal acceleration of the center of gravity	in/sec^2
g	Local acceleration due to gravity	in/sec^2
g_o	Acceleration due to gravity at earth's surface	in/sec^2
m	Mass of vehicle	$lb\text{-}sec^2/in$
W	Vehicle weight	lbs
I	Mass moment of inertia $= \sum\limits_{o}^{\ell} m(x)\ r\ (x)^2$	$lb\text{-}in/sec^2$
A	Total aerodynamic drag	lbs
$A(x)$	Local drag	lbs/in
N	Total aerodynamic normal force	lbs
$N(x)$	Local normal force	lbs/in
T	Engine thrust	lbs
F_x, F_y	Forces acting on the vehicle in the x and y direction respectively	lbs
M_T	External rotational moment	in-lbs
n_x	Axial load factor	g's
n_y	Normal load factor	g's
$\Delta n_y(x)$	Component of normal load factor due to rotation	g's
P	Axial load	lbs

Symbol	Description	Units
V	Shear	lbs
M	Bending moment	in-lbs

Referring to Figure B-1, the equations of motion for each degree of freedom may be written by applying Newton's Second Law as

$$\Sigma F_x = T \cos\delta - A - mg \sin(\theta+\Phi) = m\ddot{x} , \qquad (B-1)$$

$$\Sigma F_y = T \sin\delta + N - mg \cos(\theta+\Phi) = m\ddot{y} , \quad \text{and} \qquad (B-2)$$

$$\Sigma M_T = N L_{cp} - T \sin\delta L_E = I\ddot{\theta} \qquad (B-3)$$

Load factors may be defined as the sum of the external forces acting on the body divided by the weight of the body or

$$n_x = \frac{\Sigma F_x \text{ (external)}}{W} , \quad \text{and} \qquad (B-4)$$

$$n_y = \frac{\Sigma F_y \text{ (external)}}{W} . \qquad (B-5)$$

If the body is angularly accelerating, there is an additional component of load factor in the y direction which may be written as

$$\Delta n_y(x) = \frac{\Sigma M_T}{I g_o} r(x) . \qquad (B-6)$$

Noting that weight is the measure of the force on a mass at the earth's surface, $m = \frac{W}{g_o}$, we may substitute Equations (B-1), (B-2) and (B-3) into (B-4), (B-5) and (B-6) as

$$n_x = \frac{T \cos\delta - A}{W} = \frac{\ddot{X}}{g_o} + \frac{g}{g_o} \sin(\theta + \Phi) \ , \qquad (B\text{-}7)$$

$$n_y = \frac{T \sin\delta + N}{W} = \frac{\ddot{Y}}{g_o} + \frac{g}{g_o} \cos(\theta + \Phi) \ , \quad \text{and} \qquad (B\text{-}8)$$

$$\Delta n_y(x) = \frac{NL_{cp} - T \sin\delta \ L_e}{Ig_o} \ r(x) = \frac{\ddot{\theta}}{g_o} \ . \qquad (B\text{-}9)$$

Either part of these equations may be used in the determination of load factor. Since it is more convenient to work with force along the vehicle axis and with angular accelerations instead of axial and normal accelerations, external moments, and space angles, the following longitudinal and normal load factor definitions are generally used

$$n_x = \frac{T \cos\delta - A}{W} \ , \quad \text{and} \qquad (B\text{-}10)$$

$$n_y(x) = \frac{T \sin\delta + N}{W} + \frac{\ddot{\theta}}{g_o} \ r(x) \ . \qquad (B\text{-}11)$$

However, since a constant attitude control law is employed in this memorandum, the angular acceleration term in B-11 drops out and the equation for the normal load factor becomes

$$n_y(x) = \frac{T \sin\delta + N}{W} \ . \qquad (B\text{-}12)$$

2.0 WEIGHT DISTRIBUTION/NORMAL AND AXIAL FORCE COEFFICIENTS

The determination of flight bending moments, shears, and axial loads requires a knowledge of structure weights, propellant weights, and the distribution of concentrated loads as well as airloads at max q.

Referring to Figures 1 and 2 in the memorandum which depict the low cost launch vehicle/bulbous and lifting body payload configurations, the corresponding weight distributions of the various components as used in this analysis are shown in

Tables B-1 and B-2. Components, weights, and station locations are listed for the max q loading condition (82 seconds after liftoff).

2.1 Normal and Axial Force Coefficients

The normal force distribution on the vehicle at max q is a function of airframe geometry, angle of attack and Mach number. The resultant normal force and its location produces the aerodynamic moment which requires the thrust vector of the engine to rotate in compensating for attitude deviations.

The axial force distribution depends only on geometry and Mach number for a limited range of angle of attack (near zero degrees). The axial force can be separated into two parts: (1) pressure and skin function drag; and, (2) base drag. They both add directly to the structural axial loads on the vehicle.

Figures B-2 and B-3 depict the local normal and axial force coefficient distribution (ΔC_N, ΔC_A) for the bulbous and lifting body payload configurations with which the external aerodynamic loading can be defined. These coefficients correspond to an angle of attack of 5 degrees. The total axial force coefficients as well as the total normal force coefficients and their centers of pressure are cited for these configurations. These coefficients were derived from data listed in References 5 and 9. Using these coefficients, local normal and axial aerodynamic forces can be determined as

$$\Delta N = \Delta C_N \, qS \, , \quad \text{and} \qquad\qquad (B\text{-}13)$$

$$\Delta A = \Delta C_A \, qS \, , \qquad\qquad (B\text{-}14)$$

where S is a reference cross-section area equal to 1260 ft^2 (first stage diameter = 40 ft), and q is the maximum aerodynamic pressure (including gusts) at max q (equal to 689 psf). The total normal and axial aerodynamic loadings are correspondingly

$$N = C_N \, qS \, , \quad \text{and} \qquad\qquad (B\text{-}15)$$

$$A = C_A \, qS \, . \qquad\qquad (B\text{-}16)$$

TABLE B-1

WEIGHT DISTRIBUTION FOR LCLV BULBOUS PAYLOAD CONFIGURATION AT MAX q

COMPONENTS	WEIGHT (LBS)	STATION (FT)	
LAUNCH ESCAPE SYSTEM	8,200	390.1	
COMMAND MODULE	13,000	368.7	
STRUCTURE	12,100	359.6	BULBUS PAYLOAD
PROPELLANT	8,900	357.3	
SERVICE MODULE/LUNAR MODULE ADAPTER	3,800	335.7	
PROPELLANT	50,000	318	
SHELL	4,000	310.8	
		298	
ASTRIONICS	693	297.0	
OXIDIZER	215,398	292.0	
TANKS & SKIRTS, PRESS. SYS, ROLL & ULLAGE CONTROL	26,833	287.0	STAGE 3
FUEL	107,699	281.0	
LITVC	646	276.0	
ENGINES & VALVES	6,132	264.4	
INTERSTAGE	14,122	258.5	
		241	
ASTRIONICS	529	240.0	
OXIDIZER	1,051,157	229.5	
TANKS & SKIRTS, PRESS. SYS, ROLL & ULLAGE CONTROL	130,705	220.0	
CONTINGENCY	18,958	219.5	STAGE 2'
FUEL	525,578	209.0	
LITVC	3,153	201.0	
ENGINES & VALVES	23,655	180.0	
INTERSTAGE	84,884	170.0	
		140	
ASTRIONICS	2,099	139.0	
TANKS & SKIRTS, PRESS. SYS, ROLL & ULLAGE CONTROL OXIDIZER	1,758,635	99.5	
CONTINGENCY	73,994	86.7	STAGE 1
LITVC, FUEL	641,729	64.0	
ENGINES & VALVES	100,483	39.4	

TABLE B-2

WEIGHT DISTRIBUTION FOR LCLV/LIFTING BODY PAYLOAD CONFIGURATION AT MAX q

COMPONENTS	WEIGHT (LBS)	STATION (FT)	
			LIFTING BODY PAYLOAD
LIFTING BODY PAYLOAD	94,060 ⟶	327.3	
PAYLOAD ADAPTER	5,940 ⟶	302.0	
		———— 298	
ASTRIONICS	693 ⟶	297.0	
OXIDIZER	215,398 ⟶	292.0	
TANKS & SKIRTS, PRESS. SYS, ROLL & ULLAGE			
CONTROL	26,833 ⟶	287.0	STAGE 3
FUEL	107,699 ⟶	281.0	
LITVC	646 ⟶	276.0	
ENGINES & VALVES	6,132 ⟶	264.4	
INTERSTAGE	14,122 ⟶	258.5	
		———— 241	
ASTRIONICS	529 ⟶	240.0	
OXIDIZER	1,051,157 ⟶	229.5	
TANKS & SKIRTS, PRESS. SYS, ROLL & ULLAGE			
CONTROL	130,705 ⟶	220.0	STAGE 2
CONTINGENCY	18,958 ⟶	219.5	
FUEL	525,578 ⟶	209.0	
LITVC	3,153 ⟶	201.0	
ENGINES & VALVES	23,655 ⟶	180.0	
INTERSTAGE	84,884 ⟶	170.0	
		———— 140	
ASTRIONICS	2,099 ⟶	139.0	
TANKS & SKIRTS, PRESS. SYS, ROLL & ULLAGE			
CONTROL OZIDIZER	1,758,635 ⟶	99.5	STAGE 1
CONTINGENCY	73,994 ⟶	86.7	
LITVC, FUEL	641,729 ⟶	64.0	
ENGINES & VALVES	100,483 ⟶	39.4	

$\Delta C_A = 0.089$

351.3' $\rightarrow \Delta C_N = 0.0495$

323.6'

314.85' $\rightarrow \Delta C_N = 0.0132$

$\Delta C_A = 0.0047$

298'

296.35' $\rightarrow \Delta C_N = 0.0045$

278'

$\Delta C_A = 0.0661$

252.7' $\rightarrow \Delta C_N = 0.058$

241'

235.45' $\rightarrow \Delta C_N = 0.0135$

$\Delta C_A = 0.008$

207.8' $\rightarrow \Delta C_N = 0.0078$

203'

$\Delta C_A = 0.050$

160' $\rightarrow \Delta C_N = 0.074$ $\rightarrow$ TOTAL $C_N = 0.373$

157'

140'

127.7' $\rightarrow \Delta C_N = 0.0117$

NOTE:
ANGLE OF ATTACK = 5°

$\Delta C_A = 0.0143$

99.8' $\rightarrow \Delta C_N = 0.0099$

77' $\rightarrow \Delta C_N = 0.0016$

63'

TOTAL $C_A = 0.8378$

$\Delta C_A = 0.600$

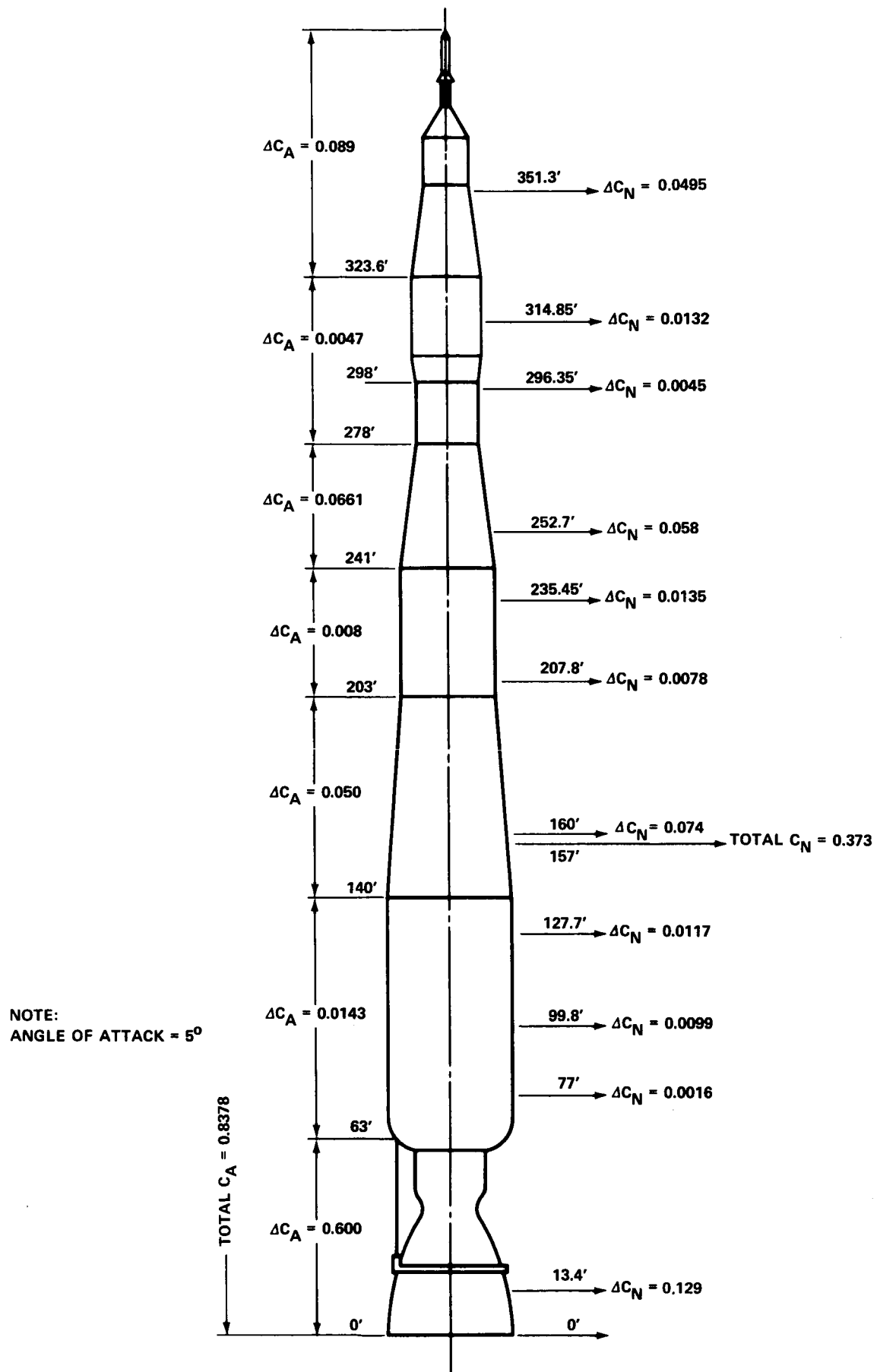13.4' $\rightarrow \Delta C_N = 0.129$

0'   0'

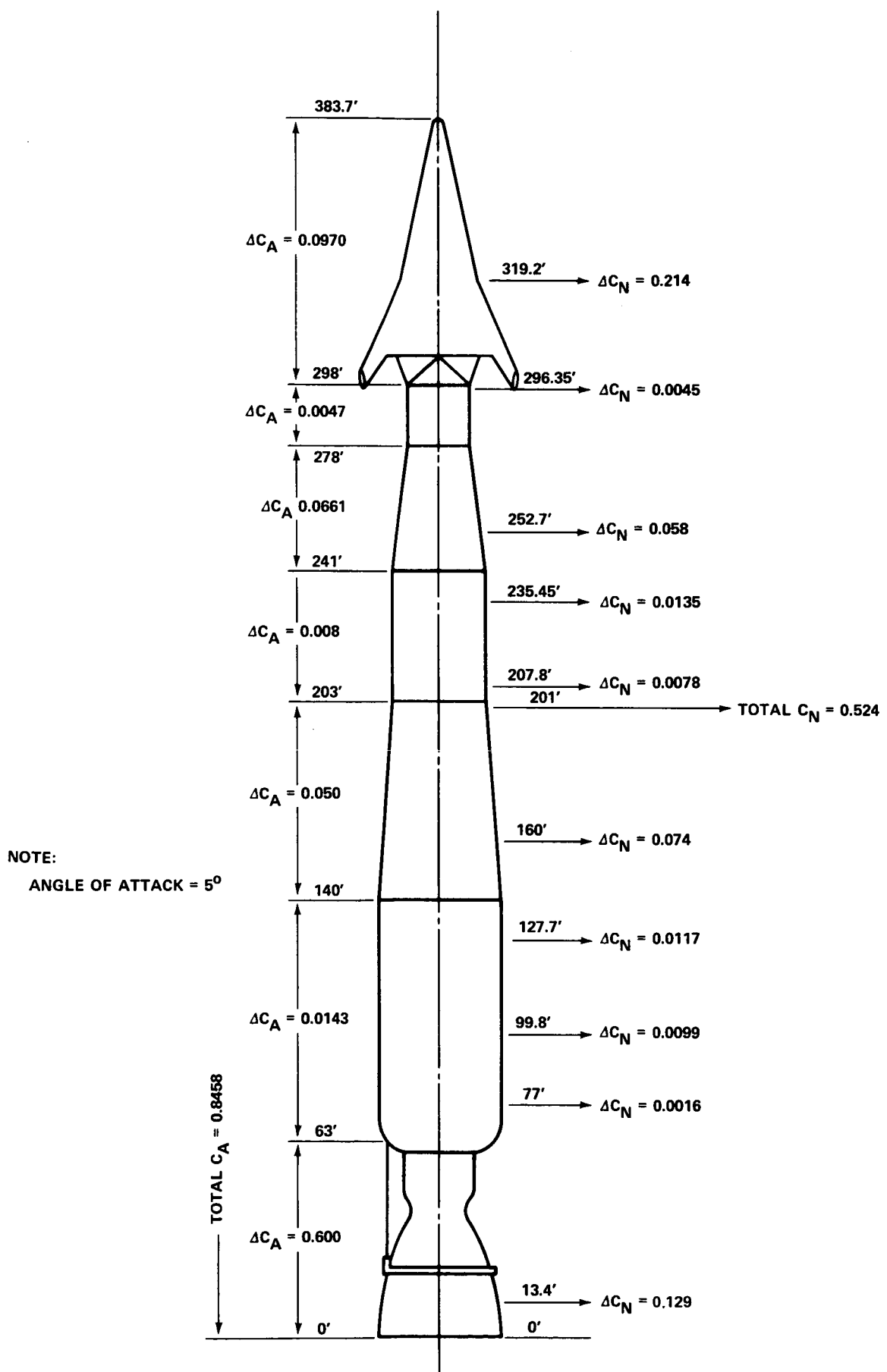FIGURE B-2 - LCLV BULBOUS PAYLOAD NORMAL AND AXIAL FORCE COEFFICIENTS

FIGURE B-3 - LCLV/LIFTING BODY PAYLOAD NORMAL AND AXIAL FORCE COEFFICIENTS

3.0 LOAD DETERMINATION

Using Equations (B-10) and (B-12), the weight distributions in Tables B-1 and B-2, and the normal and axial force coefficients as cited in Figures B-1 and B-2, the vehicle rigid body loading condition can now be determined. Through the application of D'Alembert's principle it is possible to reduce the problem in kinetics to an equivalent problem in statics by introducing appropriate inertia forces. These inertia forces find their inception in the accelerated masses of structure, subsystems, and propellant.

The axial and normal load factors for the bulbous payload and lifting-body payload vehicle configurations are determined from Equations (B-10) and (B-12) as follows:

For the bulbous payload/launch vehicle configuration the thrust vector angle $\delta=0$ since the CG and CP are coincident. Therefore, Equations (B-10) and (B-12) reduce to

$$n_x = \frac{T-A}{W} , \quad \text{and} \tag{B-17}$$

$$n_y = \frac{N}{W} . \tag{B-18}$$

At 82 seconds after liftoff (max q)

W = 4,887,082 lbs,

T = 13,788,100 lbs,

N = (0.3730) (689) (1260) = 324,000 lbs, and

A = (0.8378) (689) (1260) = 727,000 lbs.

Substituting these values into Equations (B-17) and (B-18)

$$n_x = 2.67 , \quad \text{and}$$

$$n_y = 0.0664 .$$

For the lifting body/launch vehicle configuration the CG and CP of the total vehicle are not coincident. Therefore, the angle δ must be determined. Summing the moments about the vehicle

CG (See Figure 2)

$$T \sin\delta(157-63) - N(201-157) = 0, \text{ and}$$

$$\delta = \sin^{-1}(0.468\frac{N}{T}). \tag{B-19}$$

At 82 seconds after liftoff (max q)

$W = 4,887,082$ lbs,

$T = 13,788,100$ lbs,

$N = (0.5240)(689)(1260) = 455,000$ lbs, and

$A = (0.8458)(689)(1260) = 734,000$ lbs.

Substituting these values into Equations (B-19), (B-10) and (B-12),

$\delta = 53.2'$,

$n_x = 2.67$ (same as bulbous configuration), and

$n_y = 0.137$ (significantly different from bulbous configuration).

Multipyling the vehicle weights, as listed in Tables B-1 and B-2 by the normal load factors n_y and accounting for the angle required of the thrust vector to maintain constant attitude during max q winds, the moment diagrams for inertia relief loadings can readily be determined. Inertia-relief moment diagrams for both launch vehicle/payload configurations are shown in Figures 5 and 9 in the memorandum.

Using Equation (B-13), the aerodynamic normal force distributions can also readily be determined. Aerodynamic moment diagrams for both launch vehicle/payload configurations are plotted together with the corresponding inertia relief moments on Figures 5 and 9. The resulting cross-sectional launch vehicle moment at any station is, therefore, the difference between the aerodynamic and inertia-relief moments.

Using the same general approach as above, the axial aerodynamic and inertia loadings are calculated and plotted in Figures 6 and 10 in the memorandum for both launch vehicle/ payload configurations. However, the resulting axial load at

any launch vehicle station is now the summation of the two curves, not the difference.

4.0 EVALUATION OF CRITICAL LOADING CONDITIONS

The evaluation of critical design loading conditions involves a combination of a number of parameters: (1) axial load, (2) bending moment, (3) temperature, (4) factor of safety, and (5) other items such as internal pressure, local dynamic pressure, etc. In many cases it is extremely difficult to point to the one item that definitely labels a particular condition as "critical". The selection of the critical condition can be made easier by first combining some of the above parameters into one parameter that represents an ultimate loading condition. This may be done in the following manner:

$$P_{eq} = FS \left[\frac{|M|}{\pi R^2} + \frac{|P|}{2\pi R} + p \frac{r(x)}{2} \right] \tag{B-20}$$

where

$\qquad$ FS = Factor of safety,

$\qquad$ p = Internal pressure, and

$\qquad$ R = Station radius.

The symbol P_{eq} represents an equivalent ultimate running load around the circumference of the launch vehicle structure which, when combined with temperature, can determine critical flight conditions. In this analysis, appropriate values for the factor of safety, internal pressure and temperature were not considered since the relative effect in loading for the two LCLV/payload configurations is required for scaling weights and it is assumed that the same conditions apply in each case.

Plots of P_{eq} loadings for both launch vehicle/payload configurations are shown in Figures 8 and 11 of the memorandum. It is seen that the effect of a lifting body payload becomes more pronounced towards the forward end of the vehicle. This effect results from the greater bending moments produced by the lifting body at max q.

BELLCOMM, INC.

APPENDIX C

ANALYSIS OF MAXIMUM LONGITUDINAL LOADS

The maximum longitudinal launch load experienced by the LCLV occurs just before first stage engine cutoff. The vehicle is essentially in a vacuum at this point of the trajectory and therefore senses a negligible amount of aerodynamic drag. Also, since the vehicle is undergoing a gravity turn with no disturbances from winds, the thrust vector is in line with the longitudinal axis.

The thrust to weight ratio, or number of axial g's experienced by the vehicle just before first stage engine cutoff can be determined from the equation.

$$\frac{T_h}{W_h} = \frac{1}{W_h}(T_{SL} + P_{SL}\, A_e) \, , \qquad\qquad (C-1)$$

where

T_h = thrust at altitude (lbs),

T_{SL} = thrust at sea level = 11,523,150 lbs,

P_{SL} = pressure at sea level = 2,120 psf,

A_e = exit area of first stage engine = 1,260 ft^2, and

W_h = total vehicle weight at first stage engine cutoff = 2,999,320 lbs.

Substituting these values into Equation (C-1), the thrust to weight ratio just before first stage engine cutoff is

$$\frac{T_h}{W_h} = 4.73 \text{ g's} \, .$$

Knowing the maximum axial g load experienced during flight, the distribution of maximum longitudinal loading can readily be determined. A plot of this distribution for the LCLV is shown in Figure 7 of the memorandum.

BELLCOMM, INC.

APPENDIX D

PAYLOAD PENALTY ANALYSIS

Nomenclature

μ_3 = mass ratio for third stage burn

   = initial gross weight/burnout gross weight = 3.41

W_I = inert weight of third stage

W_i = forward interstage weight (between second and third stage)

ΔW_i = increase in interstage weight = 2,658 lbs

W_p = propellant weight of third stage

ΔW_p = reduction in third stage propellant weight

W_{PL} = payload weight

ΔW_{PL} = reduction in payload weight

A structural weight penalty is incurred in the forward interstage of the three-stage TRW LCLV due to launching a lifting body payload instead of a bulbous payload. To determine the effect of this penalty on payload capability, ΔV stage capabilities (velocity increments) are assumed to remain unchanged. Based on this assumption, the payload penalty relationship can be derived from the conditions:

1. the total weight of the payload, third stage and forward interstage are constant (ΔV's for first and second stages remain unchanged), and

2. the third stage mass ratio is constant (third stage ΔV remains unchanged).

Condition 1
<u></u>

The total weight of the payload, third stage and forward interstage can be equated as

$$W_{PL} + W_I + W_P + W_i = W_{PL} - \Delta W_{PL} + W_I + W_P - \Delta W_P + W_i + \Delta W_i$$

or

$$\Delta W_i - \Delta W_P - \Delta W_{PL} = 0. \qquad (D-1)$$

Condition 2
<u></u>

Two equations can be written for the mass ratio as

$$\mu_3 = \frac{W_I + W_P + W_{PL}}{W_I + W_{PL}} \qquad (D-2)$$

and

$$\mu_3 = \frac{W_I + W_P - \Delta W_P + W_{PL} - \Delta W_{PL}}{W_I + W_{PL} - \Delta W_{PL}} \qquad (D-3)$$

From Equation (D-2)

$$(W_I + W_{PL}) \mu_3 = W_I + W_P + W_{PL}. \qquad (D-4)$$

Substituting Equation (D-4) into (D-3)

$$\mu_3 = \frac{(W_I + W_{PL}) \mu_3 - \Delta W_P - \Delta W_{PL}}{W_I + W_{PL} - \Delta W_{PL}}$$

and

$$\Delta W_P = \Delta W_{PL} \mu_3 - \Delta W_{PL}. \qquad (D-5)$$

From Equations (D-5) and (D-1), the payload penalty relationship is determined to be

$$\Delta W_{PL} = \frac{\Delta W_i}{\mu_3} .$$

$$(D-6)$$

Substituting the values for ΔW_i and $\bar{\mu}_3$ into Equation (D-6), the associated payload penalty is

$$\Delta W_{PL} = 780 \text{ lbs} .$$